Analysis of the Land Use and Cover Changes in the Metropolitan Area of Tepic-Xalisco (1973–2015) through Landsat Images

Armando Avalos Jiménez [1,*], Fernando Flores Vilchez [2], Oyolsi Nájera González [2] and Susana M. L. Marceleño Flores [2]

1   Posgrado en Ciencias Biológico Agropecuarias, Unidad Académica de Agricultura, Universidad Autónoma de Nayarit (Autonomous University of Nayarit), Carretera Tepic-Compostela Km 9, Xalisco C.P. 63780, Nayarit, México
2   Secretaría de Investigación y Posgrado, Universidad Autónoma de Nayarit, Ciudad de la Cultura s/n, Col. Centro, Tepic C.P. 63000, Nayarit, Mexico; vilchez@hotmail.com (F.F.V.); oyolsi92@gmail.com (O.N.G.); smlmarcel@hotmail.com (S.M.L.M.F.)
*   Correspondence: armand18_a@hotmail.com; Tel.: +52-311-122-88-48

check for updates

Abstract: Land use and cover changes (LUCC) have been identified as one of the main causes of biodiversity loss and deforestation in the world. Fundamentally, the urban land use has replaced agricultural and forest cover causing loss of environmental services. Monitoring and quantifying LUCC are essential to achieve a proper land management. The objective of this study was to analyze the LUCC in the metropolitan area of Tepic-Xalisco during the period 1973–2015. To find the best fit and obtain the different land use classes, supervised classification techniques were applied using Maximum Likelihood Classification (MLC), Support Vector Machines (SVMs) and Artificial Neural Networks (ANNs). The results were validated with control points (ground truth) through cross tabulation. The best results were obtained from the SVMs method with kappa indices above 85%. The transition analysis infers that urban land has grown significantly during 42 years, increasing 62 km^2 and replacing agricultural areas at a rate of 1.48 km^2/year. Forest loss of 5.78 km^2 annually was also identified. The results show the different land uses distribution and the dynamics developed in the past. This information may be used to simulate future LUCC and modeling different scenarios.

Keywords: Maximum Likelihood Classification; Support Vector Machines; Artificial Neural Networks; significant transitions; urban growth; Nayarit (Mexico)

1. Introduction

Terrestrial ecosystems are important components of nature since they have biological and functional effects on climate regulation, the hydrologic cycle and as a source of natural resources to satisfy human needs. However, during the last 300 years, the planet has suffered big transformations [1]. The ecosystems have been subject to accelerated processes of land use and cover changes (LUCC) [2], which have been identified as one of the main factors contributing to global environmental change [3–5], as a result of major current environmental problems [6] such as land loss and degradation, climate change, biodiversity loss, deforestation [7] and ecosystems fragmentation [4,8,9], which in turn cause loss of associated environmental services [10] to such a degree that more than half of the world's forest cover has been lost, and around 30% of these ecosystems face degradation processes. Anthropogenic activities are one of the main elements that contribute to land use changes [11].

Mexico is known as a megadiverse country, consisting of large diversity of organisms, landscapes and terrestrial ecosystems [12]. Forests, jungles and other natural vegetation are distributed all

over the country [13] covering 74% of the national territory [14], about 146 million hectares [12]. The distribution of natural vegetation has been studied for monitoring LUCC, but most of the research conducted at a regional scale has focused on the analysis of losses in natural vegetation and deforestation [15,16]. The deforestation rates recorded show a difference from 260,000 ha/year to 775,000 ha/year (i.e., 2600 km^2/year to 7760 km^2/year) [15]. Since local scale studies on LUCC have been scarce [14], the present work was centered on monitoring LUCC locally, paying particular attention to the urban land use in the metropolitan area of Tepic-Xalisco as a starting point for further research on urban growth simulation and future scenarios design.

The advance in using Geographic Information Systems (GIS) and remote sensing techniques has proven to be very useful to get accurate and coherent information according to the spatial reality [16]; these tools are widely used to analyze the distribution, patterns and trends of the LUCC processes via different methods to obtain several land use classes in the territory, as well as diverse approaches to detect temporary differences, such as the traditional method of cross tabulation [17,18].

In this context, the objective of this study was to analyze the dynamics on urban LUCC at local scale. The methodology was developed through the analysis and processing of four Landsat satellite images corresponding to the years 1973, 1985, 2000 and 2015. To find the best fit and obtain the different land use classes, three supervised classification methods were applied: Maximum Likelihood Classification (MLC), Support Vector Machines (SVMs) and Artificial Neural Networks (ANNs). The results were validated with control points (ground truth). Then, to identify the significant transitions between different land uses—especially in the urban land use changes—losses, gains, changes and interchanges were obtained through the cross-tabulation matrix and according to the methodology of Pontius [19].

The remainder of the paper is organized into four sections. Section 2 describes the study area and the satellite images that were used to obtain different classes of cover and land use. Section 3 outlins the procedure that was followed to classify the satellite images using two supervised classification methods and LUCC analysis. Section 4 describes and discusses the results obtained with respect to other similar works. Finally, the conclusions are presented in the Section 5.

2. Materials and Methods

2.1. Study Area

The metropolitan area of Tepic-Xalisco is located in the central part of the state of Nayarit (Mexico), as presented in Figure 1. The study area comprises two of the main localities of the state that are linked by commercial and administrative activities through the Tepic-Xalisco highway, which in turn provoked a conurbation process that was formalized as metropolitan area in 2006 by the National Institute of Statistics and Geography (INEGI, for its abbreviation in Spanish), the National Population Council (CONAPO, for its abbreviation in Spanish) and the Ministry of Social Development (SEDESOL, for its abbreviation in Spanish).

The study area was delimited through a 900 km^2 quadrant (30 km × 30 km polygon) including the metropolitan area, a polygon wide enough to locally observe and analyze the processes of LUCC during a 42 year-period.
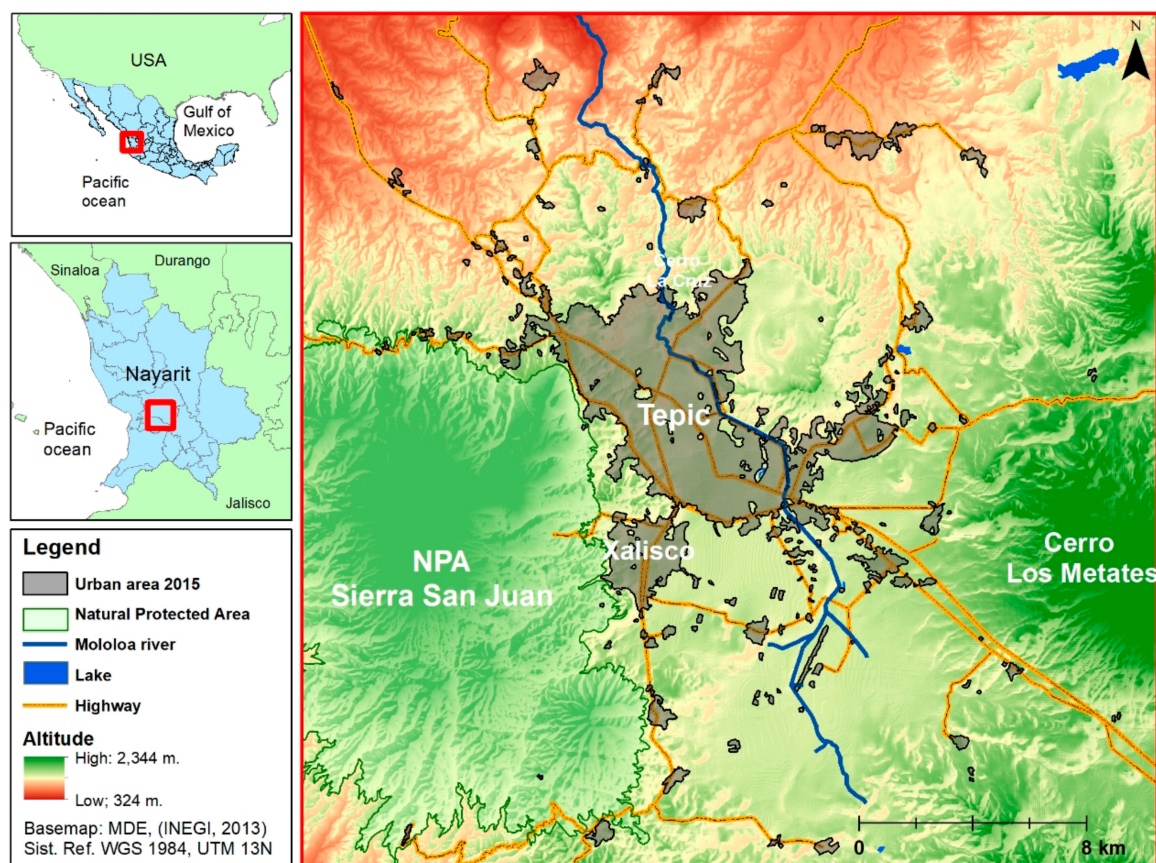
Figure 1. Localization and delimitation of the study area. Source: Own elaboration based on INEGI's data.
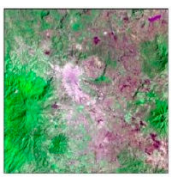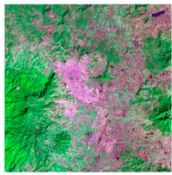
The surrounding zone of the study area contains a diversity of land use where are predominant intensive agricultural activities—mainly devoted to sugarcane, maize, mango and jicama crops—as well as farming activities. To the West of the study area is located the Natural Protected Area (NPA) Sierra de San Juan with over 50% of cover consisting of pine trees and live oaks forest, a great variety of natural resources that provide diverse environmental services susceptible of exploitation.

The metropolitan area has suffered important changes in land use as a result from urban growth. The forest is endangered by the indiscriminate clearcutting activities and mining performed in the east of the mountain, at the boundaries of the locality of Xalisco. Therefore, a historical analysis is necessary to show the distribution of land use and the change processes during a period of 42 years. Such information may be used to simulate future land use changes, such as the urban growth and modeling several scenarios.

2.2. Data

To set a temporary standardized thematic nomenclature for the analysis of the different land use, the four Landsat satellite images described in Table 1 were used. The images were taken from the United States Geological Survey (USGS) official website (http://glovis.usgs.gov).

Table 1. Landsat images used for mapping land uses in the study area.

Description	Image	Description	Image
Landsat 1 (1973) Multispectral Scanner System (MSS) Sensor LM10320451973043GDS03 Scene Spatial resolution 60 m Acquisition date 12 February 1973 Composition V-A-R		Landsat 5 (1985) Thematic Mapper (TM) Sensor LT50300451985139AAA03 Scene Spatial resolution 60 m Acquisition date 5 May 1985 Composition NIR-SWIR-R	
Landsat 7 (2000) Enhanced Thematic Mapper (ETM) Sensor LE70300452000045EDC00 Scene Spatial resolution 30 m Acquisition date 14 February 2000 Composition NIR-SWIR-R		Landsat 8 (2015) Operational Land Imager (OLI) Sensor LO80300452015062LGN01 Scene Spatial resolution 30 m Acquisition date 3 April 2015 Composition NIR-SWIR-R	

Source: United States Geological Survey (USGS) official website.

2.3. Methodology

Figure 2 shows the methodological process that was followed to analyze urban land use changes in the metropolitan area during a period of 42 years. First, supervised classification techniques were applied through Maximum Likelihood Classification (MLC), Support Vector Machines (SVMs) and Artificial Neural Networks (ANNs); from the preparation of the images (pre-processing) to the application of three supervised classification methods (processing), and validation of classifications (post-processing). Then, to detect changes between different land uses, the periods 1973–1985, 1985–2000, 2000–2015 and 1973–2015 were analyzed using cross tabulation. Finally, to identify significant changes, transitions analysis was conducted using the method of Pontius [19]. All processes were performed using GIS with ENVI 5.3, Arcgis 10.3 and Focus (PCI Geomatics, 2015) applications.
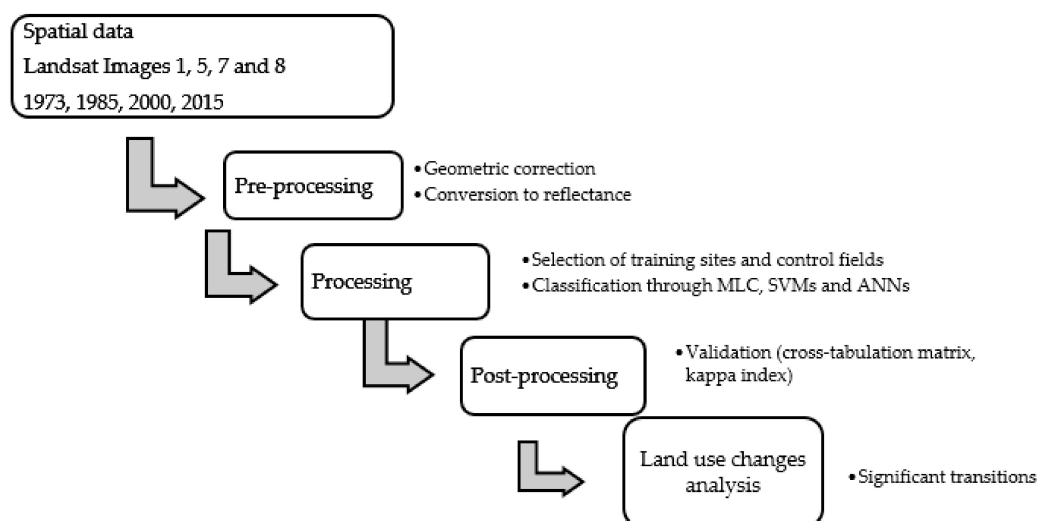

Figure 2. Landsat images classification methodology for LUCC analysis. Source: Own elaboration.

3. Satellite Images Classification

3.1. Pre-Processing

The scenes of Landsat images 1, 5, 7 and 8 were pre-processed to classify the different types of land use during the identification of changes in the urban areas for each analyzed period. Prior to images processing, the study area was cropped for each satellite image by means of a layer (30 km × 30 km polygon) wide

enough to visualize urban land use changes in the metropolitan area during a 42-year period; the polygon was measured from the center of the urban land of the metropolitan area.

In the region of interest, it was necessary to verify and standardize the pixel size and the dimensions of each image by means of geometric correction in the WGS-1984 reference system, UTM projection in the zone 13 N. The validation of the geometric correction was obtained with the Mean Squared Error (MSE) for the control points, using one of the images as reference and comparing it (in pairs) to get the best geometric adjustment. To standardize a spatial resolution to 30 m, the four Landsat images were standardized by resampling the pixel size, especially the 1 and 2 Landsat images.

Spectral bands were selected for each image, in particular the ones with optical spectrum, Near Infrared (NIR) and Short-Wave Infrared (SWIR); the panchromatic bands were omitted due to high atmospheric influence, as well as the thermal bands, especially in the 7 and 8 Landsat images. To easily visualize the several classes of covers and land uses, a RGB composition in false color was used, highlighting the strong green areas with the NIR, SWIR and R combination; in addition, 2% of linear contrast highlighting was applied to enhance the visualization and identification of the training sites.

The conversion to reflectance was performed to obtain the terrestrial area spectral reflectance values for the different covers and land uses, giving the spectral value to each pixel. The conversion to reflectance was conducted considering the method of Chavez [20] through the following equation (Equation (1)).

$$\rho_k = \frac{d^2 * \pi * \partial_{1,k} * (ND_k - ND_{min,\,k})}{E_{0,k} * sin\,\theta_e * \tau_{k,i}} \tag{1}$$

where ρ_k is the reflectance for the k band; d is the factor that considers the solar variation from the Earth–Sun distance, calculated from the Julian Day; $\partial_{1,k}$ is the conversion to radiance multiplicative coefficient; θ_e is the solar elevation angle; and $E_{0,k}$ is the solar irradiance in the top of atmosphere for the k band. The data to make the conversion to reflectance were obtained from the header files of each satellite image.

3.2. Processing

For processing the images, spectral signatures were created from selecting training sites based on the identification of similar areas in different covers and land uses, combining the knowledge of the area for a proper selection of the regions of interest (ROI). To identify the different land use classes, some visual patterns such as tone, texture and the influence areas were used.

During the identification of the training sites, the separability of the spectral signatures was verified for the five land use classes described in Table 2.

Table 2. Description of identified covers and land uses.

Class No.	Class	Description
1	Urban	Includes urban and industrial areas.
2	Agricultural	Periodic and temporary irrigation agriculture.
3	Water bodies	Water bodies, lakes and rivers.
4	Secondary vegetation	Includes arbustive (scrub and grassland) and arboreal vegetation of low or scarce density.
5	Forest	High density arboreal vegetation.

Source: Own elaboration.

While selecting the training sites, control fields verified in situ were also set for validation of each classified image (post-processing).

To obtain the different land use classes, three supervised classification methods were used. First, the Maximum Likelihood Classification (MLC) method, as the most widely used in the scientific literature, is fast, easy to apply and enables a clear interpretation of the results [21]. This algorithm can

obtain a spectral image of each land use class through variance and covariance statistics of the set of training sites identified in the image and calculates the probability of belonging to each class according to the spectral signature; this method has been proven in works such as those of [22–25], with satisfactory results.

The Support Vector Machines (SVMs) algorithm was the second method applied. This automatic learning algorithm trains linear and non-linear learning functions by transforming the original data into a different space with a function (kernel) to obtain the hyperplane which maximizes the margin of separation between two or more classes to be classified [26]. Currently, the SVMs algorithm is among the most reliable methods; therefore, it is used in many works [27–29] with satisfactory results. For the classification of images the Radial Basis Function (RBF) for not-linearly separable data was used.

Finally, the third method applied was the Artificial Neural Networks (ANNs), an automatic learning method that predicts a complex behavior from a sample of observed inputs and outputs. The network structure is based on a simplified model of the human brain consisting of three layers: input, hidden and output. This structure is trained to recognize the result from input values and classify the rest according to the given rules [30,31]. Neural networks have been applied to classify satellite images with good results [32,33].

The ANNs classification was applied with a hidden layer of standard backpropagation for supervised learning by means of the logistic activation function for non-linear classification.

3.3. Post-Processing

To obtain a better representation of the land use mapping, each classified image was subject to a series of auxiliary processes: a process of majority filtering (3 × 3 pixels) and a method of generalization of polygons less than one hectare—as they are few representatives with respect to the minimum mapping unit—were applied, which reduced the image noise and eliminated the isolated polygons, resulting in the land use mapping for each year of analysis. Finally, to standardize and confirm the location of urban areas, a visual inspection of the mapped urban localities and the population census with historical data from INEGI for the same analyzed periods was carried out.

To validate the obtained results, the classified images were compared against the control fields through a cross-tabulation matrix for the different dates. At the same time the following were obtained: the kappa index, which shows the degree of similarity between a set of control fields and the classified image; the general accuracy, which indicates the percentage of pixels properly classified; the percentage of producer's accuracy, which sets the percentage of a kind of particular land use change correctly classified in the image; and the percentage of user's accuracy, which provides the percentage of a land use class in the image that matches with the class that corresponds in the land.

The model validated as the one with higher accuracy was used to represent the cover and land use mapping for the years 1973, 1985, 2000 and 2015.

3.4. Analysis of Land Use and Cover Changes

The analysis of LUCC was conducted through the cross-tabulation matrix to obtain losses, gains and interchanges between the different covers and land uses and after that, the significant transitions analysis was conducted according to the methodology proposed by [19]. For each cover and land use the cross-tabulation matrix enables to obtain, through the diagonal values, the stable areas between two dates, as well as the losses (below the diagonal) and the gains (above the diagonal). Such significant transitions on each cover and land use were obtained by comparing the gains and/or real losses against the gains and/or expected losses randomly, divided by the gains and/or expected losses. This comparison gave as a result the transition index where the values less than one indicated non-significant changes among covers and land uses, while the positive values more than one, indicated significant transitions.

4. Results and Discussion

4.1. Satellite Images Classification

Figure 3 shows the mapping of covers and land uses obtained for each classified Landsat image. The urban land use has mainly replaced agricultural land use where the productive activities has been focused on sugarcane, maize, mango and jicama crops at rate of 1.48 km^2/year.
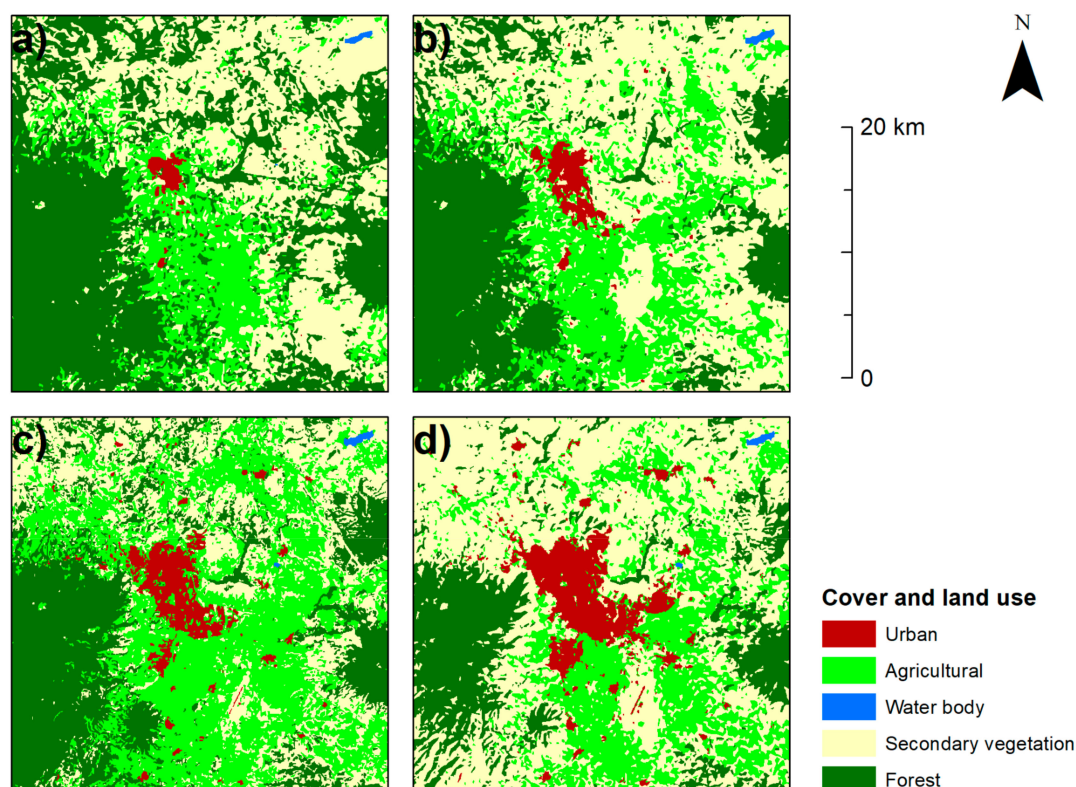

Figure 3. Image classified from Landsat images 1, 5, 7 and 8 with SVMs; Cover and land use: (**a**) 1973; (**b**) 1985; (**c**) 2000; and (**d**) 2015. Source: Own elaboration from Landsat images 1, 5, 7 and 8.

4.2. Classification Validation

Table 3 shows the results from the process of classified images validation through the cross-tabulation matrix and the parameters obtained: kappa index, general accuracy, producer's accuracy and user's accuracy. Validation statistics show better results when using the SVMs classification method, from which general accuracy above 85% is recorded for the four classified Landsat images 1, 5, 7 and 8, unlike the maximum likelihood classification and the artificial neural networks methods.

Table 3. Classified images validation.

Year Evaluated	SVMs		MLC		ANNs	
	General Accuracy	Kappa Index	General Accuracy	Kappa Index	General Accuracy	Kappa Index
1973	98.7%	0.98	97.7%	0.96	97.7%	0.96
1985	89.0%	0.85	92.5%	0.90	96.5%	0.95
2000	89.3%	0.85	82.1%	0.76	92.7%	0.90
2015	90.4%	0.87	86.1%	0.81	86.1%	0.81

Source: Own elaboration.

When selecting training fields, separability problems were identified between the secondary vegetation and the agricultural land use classes, which is reflected in the producer's accuracy percentage with values below 90%. The best fit was recorded when using the SVMs classification method, where the accuracy percentages average 96% for the user, and 95% for the producer; as shown in the Table 4.

Table 4. Percentages of producer's accuracy and user's accuracy.

Classified Image	Class	SVMs		MLC		ANNs	
		Producer's Accuracy (%)	User's Accuracy (%)	Producer's Accuracy (%)	User's Accuracy (%)	Producer's Accuracy (%)	User's Accuracy (%)
Landsat 1 MSS (1973)	Urban	100	100	100	100	100	100
	Agricultural	97	100	96	99	95	100
	Water body	100	100	100	100	100	100
	Secondary vegetation	100	95	100	93	100	98
	Forest	99	100	96	100	98	94
Landsat 5 TM (1985)	Urban	100	100	100	100	83	199
	Agricultural	100	100	100	100	100	98
	Water body	100	100	100	100	100	90
	Secondary vegetation	68	100	82	100	99	94
	Forest	100	74	100	83	93	100
Landsat 7 ETM (2000)	Urban	100	100	100	56	100	39
	Agricultural	100	100	93	100	89	98
	Water body	100	100	100	100	100	100
	Secondary vegetation	56	100	63	100	86	100
	Forest	100	67	100	71	100	89
Landsat 8 OLI (2015)	Urban	100	100	100	100	94	89
	Agricultural	100	80	100	94	95	84
	Water body	100	100	100	100	100	95
	Secondary vegetation	72	100	44	100	71	69
	Forest	100	96	100	76	83	93
Mean		95	96	94	94	94	96

Source: Own elaboration.

4.3. Analysis of Land Use Changes

Table 5 shows the changes in area for each class of cover and land use occurred during 1973–2015. The urban land use has increased 7% from the overall analyzed area with an annual rate of 1.48 km^2/year. At the same time, the forest cover has lost 28% of area in 42 years, with an annual rate of 5.78 km^2/year.

Table 5. LUCC during 1973–2015 according to the SVMs method.

Classification Method	Class	Description	1973		1985		2000		2015		Annual Rate (km^2)
			Area (km^2)	Area (%)	Area (km^2)	Area (%)	Area (km^2)	Area (%)	Area (km^2)	Area (%)	
SVMs	1	Urban	6.8	1	19.2	2	40.0	4	68.8	8	1.48
	2	Agricultural	151.1	17	215.1	24	342.8	38	211.3	23	1.43
	3	Water body	1.1	0	1.4	0	1.5	0	1.4	0	0.01
	4	Secondary vegetation	322.7	36	383.7	43	243.7	27	442.8	49	2.86
	5	Forest	418.3	46	280.6	31	272.1	30	175.7	20	5.78 *
MLC	1	Urban	6.8	1	19.2	2	39.9	4	68.6	8	1.47
	2	Agricultural	179.5	20	258.1	29	234.7	26	218.5	24	0.93
	3	Water body	1.2	0	1.7	0	1.4	0	1.5	0	0.01
	4	Secondary vegetation	396.0	44	319.6	36	372.7	41	401.7	45	0.13
	5	Forest	316.4	35	301.3	33	251.3	28	209.7	23	2.54 *
ANNs	1	Urban	6.8	1	19.2	2	39.9	4	68.8	8	1.48
	2	Agricultural	140.1	16	221.3	25	314.2	35	331.1	37	4.55
	3	Water body	1.1	0	2.6	0	2.1	0	1.8	0	0.02
	4	Secondary vegetation	281.2	31	413.4	46	283.6	32	284.4	32	0.08
	5	Forest	470.8	52	243.6	27	260.2	29	213.9	24	6.12 *

* Loss. Source: Own elaboration.

The annual rates of change for each class of cover and land use are shown in Figure 4. Differences were identified depending on the classification methods applied. When applying the SVMs and ANNs methods, the urban land use presented a similar trend of 1.48 km^2/year of change. The three methods recorded differences regarding agricultural land use, where the ANNs method registered a rate of 4.55 km^2/year, while the SVMs method obtained rates of 1.43 km^2/year. The secondary vegetation cover also presented important differences; while the SVMs method registered a rate of 2.86 km^2/year, the results of the MLC and ANNs methods presented a rate below 0.13 and 0.08 km^2/year, respectively. With regard to the forest, the methods SVMs and ANNs obtained similar annual rates of 5.78 and 6.12 km^2/year; the negative rate of change is due to the loss of surface.
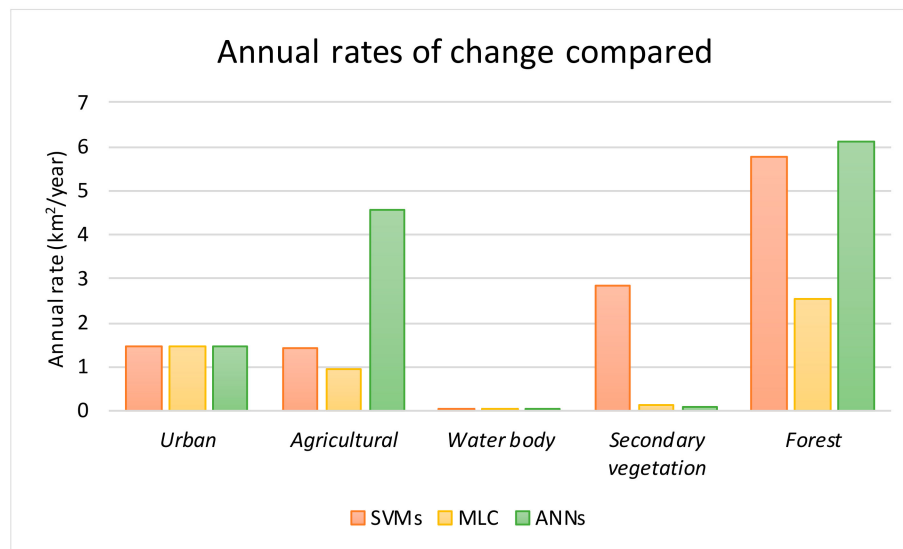

Figure 4. Annual rates of change according to the classification methods applied. Source. Own elaboration.

Since the SVMs method proved the best fit, the results from applying this method were used to analyze significant transitions and land use changes in the metropolitan area.

The changes occurred in this same period due to losses and gains are shown in Table 6. The main results show that the urban land use in the metropolitan area has increased 62 km^2 since 1973. The agricultural area and the secondary vegetation present most of the interchanges due to crop rotation, which is confirmed when observing the losses and gains of these same land use classes.

Table 6. Land use losses, gains and interchanges between periods with SVMs.

Period	Class	Area (km²)							
		Total (t1)	Total (t2)	Steady (E)	Gains (G)	Losses (L)	Interchanges (I)	Net Change (NT)	Total Change (CT)
	Urban	6.8	19.2	6.8	12.4	0.0	0.0	12.4	12.4
	Agricultural	151.1	215.1	86.6	128.5	64.5	129.0	64.0	193.0
1973–1985	Water body	1.1	1.4	1.0	0.4	0.0	0.1	0.3	0.4
	Secondary vegetation	322.7	383.7	229.0	154.7	93.7	187.4	61.0	248.4
	Forest	418.3	280.6	263.0	17.6	155.3	35.2	137.7	172.9
	Urban	19.2	40.0	19.2	20.8	0.0	0.0	20.8	20.8
	Agriculture	215.1	342.8	171.3	171.5	43.8	87.6	127.7	215.3
1985–2000	Water body	1.4	1.5	1.3	0.2	0.1	0.2	0.1	0.3
	Secondary vegetation	383.7	243.7	185.2	58.5	198.5	116.9	140.1	257.0
	Forest	280.6	272.1	227.1	45.0	53.6	90.1	8.5	98.6
	Urban	40.0	68.8	40.0	28.9	0.0	0.0	28.9	28.9
	Agricultural	342.8	211.3	182.3	29.0	160.5	58.1	131.5	189.5
2000–2015	Water body	1.5	1.4	1.3	0.1	0.3	0.2	0.2	0.4
	Secondary vegetation	243.7	442.8	203.7	239.1	40.0	79.9	199.1	279.1
	Forest	272.1	175.7	161.8	13.9	110.3	27.8	96.4	124.2
	Urban	6.8	68.8	6.8	62.0	0.0	0.0	62.0	62.0
	Agriculture	151.1	211.3	64.4	146.9	86.7	173.4	60.3	233.6
1973–2015	Water body	1.1	1.4	1.0	0.3	0.0	0.0	0.3	0.3
	Secondary vegetation	322.7	442.8	194.2	248.6	128.5	257.0	120.1	377.1
	Forest	418.3	175.7	166.4	9.3	251.9	18.5	242.7	261.1

Source: Own elaboration.

The transitions analysis for each cover and land use is summarized in Table 7. Significant transitions for the analyzed periods are registered particularly in the agricultural land use change to urban land use and secondary vegetation. The increase of urban area and secondary vegetation is because the agricultural area is being replaced. During a 42-year period, 33.1 km^2 of agricultural use transformed into urban areas and 53.3 km^2 into secondary vegetation. The forest also has been affected with transitions, although non-significant. They recorded ecological changes of 49.1 km^2 to agricultural land and 195.3 km^2 to secondary vegetation.

Table 7. Significant transitions analysis.

From	Area (km^2)				To
	1973–1985	1985–2000	2000–2015	1973–2015	
Agricultural	8.9 *	7.6 *	24.7 *	33.1 *	Urban
	0.0	0.1	0.1	0.0	Water body
	51.3 *	29.6	133.2	53.3	Secondary vegetation
	4.2	6.5	2.5	0.2	Forest
Water body	0.0	0.0	0.0	0.0	Urban
	0.0	0.0	0.1	0.0	Agricultural
	0.0	0.0	0.2	0.0	Secondary vegetation
	0.0	0.0	0.0	0.0	Forest
Secondary vegetation	2.7	12.8	3.9	21.4	Urban
	77.3	147.2	24.6	97.8	Agricultural
	0.4	0.1	0.0	0.2	Water body
	13.3	38.5	11.4	9.0	Forest
Forest	0.7	0.4	0.2	7.5	Urban
	51.2	24.3	4.4	49.1	Agricultural
	0.0	0.1	0.0	0.1	Water body
	103.4	28.8	11.4	195.3	Secondary vegetation

* Significant transition. Source: Own elaboration.

The methodology applied in this study is similar to the one used by Aguayo et al. [1], Lopez and Plata [25] and Antillón et al. [34], who applied the maximum likelihood algorithm to get the different land use classes of the study area and analyzed LUCC through cross-tabulation method or confusion matrix. The results of said investigations have had the same trend as obtained in the present study as regards to urban areas replacing agricultural lands, as well as a decrease in the forest area.

According to the scientific literature, the SVMs method has been used in several studies such as those developed by Mountrakis et al. [27]; Lu et al. [28]; and Xie et al. [29] with good results on image classification, similar to the results obtained in this work where the SVMs method registered the best fit. Some works have compared different supervised classification methods; for example, Pal and Mather [35] used the same three classification methods that were applied in this study (MLC, ANNs and SVMs), obtaining the best fit results through SVMs. On the other hand, Otukei and Blaschke [36] compared three methods of classification, MLC, SVMs and Decision Trees (DT), and affirmed that the best results were obtained when applying SVMs. In addition, Mondal et al. [37] compared the SVMs and MLC methods, and concluded that when preparing land use maps, the SVMs method is more appropriate than the MLC. Finally, in a more recent study, Wu et al. [38] compared the SVMs, ANNs and DT methods; although radial base and polynomial functions were used for SVMs, this method obtained better results with kappa indices (0.72 and 0.79 for each function, respectively). Both the results in the above mentioned research and in this work obtained the best fit applying the SVMs method; therefore, the results from applying this method were used for the LUCC analysis in the study area.

In Mexico, several studies on LUCC have been conducted to achieve a better understanding on the dynamics and processes of land use change (e.g., [2,8,14,24,25,34,39–43]). These studies have been

oriented to identify forest areas loss rates, unlike this research that was focused on analyzing the urban land use during three periods with the intention of identifying the historical dynamics of urban growth to be able to build urban growth simulation models and development of future scenarios.

Particularly, Cano et al. [44] analyzed urban land use in Hidalgo State (Mexico). From satellite images, they identified urban growth of 72.3 km^2 in a 14-year period, equivalent to an annual growth rate of 1.8%. On the other hand, by means of digital and visual techniques classification, Lopez and Plata [25] analyzed LUCC in the metropolitan area of Mexico City regarding urban expansion detecting an urban growth of 202 km^2 equivalent to 16% in a 10-year period. In comparison with the present work, in the metropolitan area of Tepic-Xalisco it was possible to quantify an urban growth of 62 km^2 during a 42-year period, with an annual rate of 1.48 km^2, which means a relatively low growth regarding to the metropolitan area of Mexico City.

For the study area, the research on cover and land use analysis conducted by Nájera et al. [45] was identified for the Mololoa River watershed, which determined natural vegetation losses of 41.67 ha/year with deforestation rates of 0.1% and urban growth of 74.86 ha/year, which is nearly half that obtained by this study that registered an increase of urban land of 148 ha/year (1.48 km^2/year). These results may be attributed to the difference in the boundaries set for the study areas, and to the methodology used to obtain the different land use classes.

5. Conclusions

The validation results from the classifications developed suggest that the SVMs method gives the best fit and offers greater certainty on the distribution and quantification of the different classes of cover and land use obtained.

The urban land use in the metropolitan area of Tepic-Xalisco has experienced an important increase within a period of 42 years, exceeding ten times the urban area recorded in 1973, with a rate of 1.48 km^2/year. This growth has produced significant changes in land use with transitions towards agricultural and secondary vegetation land use. The forest cover also has been affected, since it has experienced considerable losses of area with transformation trends towards secondary vegetation. In addition, the agricultural land use has been replaced as a result of urban growth. This situation has caused functional implications on ecosystems and to date losses of agricultural productive area are present, as well as deforestation processes.

The applied methodology enabled learning about the historical dynamics and quantifying the LUCC during a 42-year period, identifying the transitions between each land use. This information will help to establish land planning strategies, promote management and develop land use conservation policies.

References

1. Aguayo, M.; Pauchard, A.; Azócar, G.; Parra, O. Cambio del uso del suelo en el centro sur de Chile a fines del siglo XX. Entendiendo la dinámica espacial y temporal del paisaje. *Rev. Chil. Hist. Nat.* **2009**, *82*, 361–374. [CrossRef]
2. Mas, J.F.; Velázquez, A.; Reyes, D.G.J.; Mayorga, S.R.; Alcántara, C.; Bocco, G.; Castro, R.; Fernandez, T.; Perez, V.A. Assessing land use/cover changes: A nationwide multidate spatial database for Mexico. *Int. J. Appl. Earth Obs. Geoinf.* **2004**, *5*, 249–261. [CrossRef]
3. Mendoza, E.; Dirzo, R. Deforestation in Lacandonia (southeast Mexico): Evidence for the declaration of the northernmost tropical hot-spot. *Biodivers. Conserv.* **1999**, *8*, 1621–1641. [CrossRef]

4. Lambin, E.F.; Turner, B.L.; Helmut, J.; Geist, S.B.; Agbola, S.B.; Arild, A.; Bruce, J.W.; Coomes, O.T.; Dirzo, R.; Fischer, G.; et al. The causes of land-use and land-cover change: Moving beyond the myths. *Glob. Environ. Chang.* **2001**, *11*, 261–269. [CrossRef]

5. Turner, B.L.; Lambin, E.F.; Reenberg, A. The emergence of land change science for global environmental change and sustainability. *Proc. Natl. Acad. Sci. USA* **2007**, *104*, 20666–20671. [CrossRef] [PubMed]

6. Lambin, E.F.; Geist, H.J. (Eds.) *Land-Use and Land-Cover Change: Local Processes and Global Impacts*; Springer: Berlin, Germany, 2008.

7. FAO. *Evaluación de los Recursos Forestales Mundiales: Informe Nacional México*; FAO: Roma, Italy, 2010; Available online: http://www.fao.org/docrep/013/al567S/al567S.pdf (accessed on 31 May 2018).

8. Bocco, G.; Mendoza, M.; Masera, O.R. La Dinámica del Cambio del Uso del Suelo en Michoacán: Una Propuesta Metodológica para el Estudio de los Procesos de Deforestación. *Investig. Geogr.* **2001**, *44*, 18–36. Available online: http://www.redalyc.org/articulo.oa?id=56904403 (accessed on 31 May 2018). [CrossRef]

9. Velázquez, A.; Durán, E.; Ramírez, I.; Mas, J.F.; Bocco, G.; Ramírez, G.; Palacio, J.L. Land use-cover change processes in highly biodiverse areas: The case of Oaxaca, México. *Glob. Environ. Chang.* **2003**, *13*, 175–184. [CrossRef]

10. Velázquez, A.; Mas, J.F.; Díaz, G.J.R.; Mayorga, S.R.; Alcántara, P.C.; Castro, R.; Fernández, T.; Bocco, G.; Ezcurra, E.; Palacio, J.L. Patrones y tasas de cambio de uso del suelo en México. *Gaceta Ecol.* **2002**, *62*, 21–37.

11. Millennium Ecosystem Assessment. Ecosystems. 2003. Available online: https://www.millenniumassessment. org/en/index.html (accessed on 31 May 2018).

12. SEMARNAT. *Informe de la Situación del Medio Ambiente en México*; SEMARNAT: México City, México, 2012. Available online: http://apps1.semarnat.gob.mx/dgeia/informe_12/pdf/Informe_2012.pdf (accessed on 31 May 2018).

13. Challenger, A.; Soberón, J. *Los Ecosistemas Terrestres, en Capital Natural de México, vol. I: Conocimiento Actual de la Biodiversidad*; CONABIO: México City, México, 2008; pp. 87–108. Available online: http://www. biodiversidad.gob.mx/pais/pdf/CapNatMex/Vol%20I/I03_Losecosistemast.pdf (accessed on 31 May 2018).

14. Galicia, L.; García, R.A.; Gómez-Mendoza, L.; Ramírez, M.I. Cambio de uso del suelo y degradación ambiental. *Ciencia* **2007**, *584*, 50–59.

15. Mas, J.F.; Velázquez, A.; Couturier, S. La evaluación de los cambios de cobertura/uso del suelo en la República Mexicana. *Investigación Ambiental Ciencia y Política Pública* **2009**, *1*, 23–39.

16. Chuvieco, E. Teledetección Ambiental: La Observación de la Tierra Desde el Espacio (Editorial Ariel). 2008. Available online: https://drive.google.com/file/d/0B0KUmy_fthbuX09sUE9RejJJX1U/view (accessed on 31 May 2018).

17. Civco, D.L.; Hurd, J.D.; Wilson, E.H.; Song, M.; Zhang, Z. A Comparison of Land Use and Land Cover Change Detection Methods. In Proceedings of the ASPRS-ACSM Annual Conference, Washington, DC, USA, 22–26 April 2002; Available online: https://www.researchgate.net/profile/Daniel_Civco/publication/228543190_ A_comparison_of_land_use_and_land_cover_change_detection_methods/links/5570b54608aedcd33b292ec1. pdf (accessed on 31 May 2018).

18. Monjardín, A.S.A.; Pacheco, A.C.E.; Plata, R.W.; Corrales, B.G. La deforestación y sus factores causales en el estado de Sinaloa, México. *Madera y Bosques* **2017**, *231*, 7–22. [CrossRef]

19. Pontius, R.G.; Shusas, E.; McEachern, M. Detecting important categorical land changes while accounting for persistence. *Agric. Ecosyst. Environ.* **2004**, *101*, 251–268. [CrossRef]

20. Chavez, P.S. Image-based atmospheric corrections. Revisited and improved. *Photo-Gramm. Eng. Remote Sens.* **1996**, *62*, 1025–1036.

21. Bolstad, P.; Lillesand, T.M. Rapid maximum likelihood classification. *Photogramm. Eng. Remote Sens.* **1991**, *571*, 67–74.

22. Hassan, Z.; Shabbir, R.; Ahmad, S.S.; Malik, A.H.; Aziz, N.; Butt, A.; Erum, S. Dynamics of land use and land cover change (LULCC) using geospatial techniques: A case study of Islamabad Pakistan. *SpringerPlus* **2016**, *5*, 1–11. [CrossRef] [PubMed]

23. Tahir, M.; Iman, E.; Hussain, T. Evaluation of land use/land cover changes in Mekelle City. Ethiopia using Remote Sensing and GIS. *Comput. Ecol. Softw.* **2013**, *3*, 9–16.

24. García Mora, T.J.; Mas, J.F. Comparación de metodologías para el mapeo de la cobertura y uso del suelo en el sureste de México. *Investig. Geogr.* **2008**, *67*, 7–19. [CrossRef]

25. López, V.V.H.; Plata, R.W. Análisis de los cambios de cobertura de suelo derivados de la expansión urbana de la Zona Metropolitana de la Ciudad de México, 1990–2000. *Investig. Geogr.* **2009**, *68*, 85–101. [CrossRef]

26. Vapnik, V.N. *The Nature of Statistical Learning Theory*; Springer: New York, NY, USA, 1995.

27. Mountrakis, G.; Im, J.; Ogole, C. Support vector machines in remote sensing: A review. *ISPRS J. Photogramm. Remote Sens.* **2011**, *66*, 247–259. [CrossRef]

28. Lu, D.; Weng, Q.; Moran, E.; Li, G.; Hetrick, S. *Remote Sensing Image Classification*; CRC Press; Taylor and Francis: Boca Raton, FL, USA, 2011; pp. 219–240.

29. Xie, L.; Li, G.; Xiao, M.; Peng, L.; Chen, Q. Hyperspectral image classification using discrete space model and support vector machines. *IEEE Geosci. Remote Sens. Lett.* **2017**, *14*, 374–378. [CrossRef]

30. Richards, J.A. *Remote Sensing Digital Image Analysis*; Springer: Berlin, Germany, 1999; p. 240.

31. Atkinson, P.M.; Tatnall, A.R.L. Introduction Neural Networks in Remote Sensing. *Int. J. Remote Sens.* **1997**, *184*, 699–709. [CrossRef]

32. Kavzoglu, T.; Mather, P.M. The use of backpropagating artificial neural networks in land cover classification. *Int. J. Remote Sens.* **2003**, *24*, 4907–4938. [CrossRef]

33. Verbeke, L.P.C.; Vabcoillie, F.M.B.; Dewulf, R.R. Reusing back-propagating artificial neural network for land cover classification in tropical savannahs. *Int. J. Remote Sens.* **2004**, *25*, 2747–2771. [CrossRef]

34. Antillón, V.M.Y.; Corral, G.G.M.; Alatorre, C.L.C. Análisis de los Cambios de Cobertura y uso de Suelo en los Márgenes de la Laguna de Bustillos, Chihuahua: Efectos de la Expansión Agrícola. Memorias de Resúmenes en Extenso SELPER-XXI-México-UACJ-2015. 2015. Available online: http://selper.org.mx/images/Memorias2015/assets/m005.pdf (accessed on 31 May 2018).

35. Pal, M.; Mather, P.M. Support vector machines for classification in remote sensing. *Int. J. Remote Sens.* **2005**, *26*, 1007–1011. [CrossRef]

36. Otukei, J.R.; Blaschke, T. Land cover change assessment using decision trees, support vector machines and maximum likehood classification algorithms. *Int. J. Appl. Earth Obs. Geoinf.* **2010**, *12*, S27–S31. [CrossRef]

37. Mondal, A.; Kundu, S.; Chandniha, S.K.; Shukla, R.; Mishra, P.K. Comparison of support vector machine and maximum likelihood classification technique using satellite imagery. *Int. J. Remote Sens. GIS* **2012**, *1*, 116–123.

38. Wu, W.; Li, A.D.; He, X.H.; Ma, R.; Liu, H.B.; Lv, J.K. A comparison of support vector machines, artificial neural network and classification tree for identifying soil texture classes in southwest China. *Comput. Electron. Agric.* **2018**, *144*, 86–93. [CrossRef]

39. Camacho, S.J.M.; Pérez, J.; Isabel, J.; Pineda, J.N.B.; Cadena, V.E.G.; Bravo, P.L.C.; Sánchez, L.M. Cambios de cobertura/uso del suelo en una porción de la Zona de Transición Mexicana de Montaña. *Madera y Bosques* **2015**, *21*, 93–112.

40. Evangelista, O.V.; López, B.J.; Caballero, N.J.; Martínez, A.M.Á. Patrones espaciales de cambio de cobertura y uso del suelo en el área cafetalera de la sierra norte de Puebla. *Investig. Geogr.* **2010**, *72*, 23–38. [CrossRef]

41. Ramírez, R.I. Cambios en las Cubiertas del Suelo en la Sierra de Angangueo, Michoacán y Estado de México, 1971-1994-2000. *Investig. Geogr.* **2001**, *45*, 39–55. Available online: http://www.redalyc.org/pdf/569/56904504.pdf (accessed on 31 May 2018). [CrossRef]

42. Guerrero, G.; Masera, O.; Mas, J.F. Land use/land cover change dynamics in the Mexican highlands: Current situation and long-term scenarios. In *Modelling Environmental Dynamics*; Springer: Berling, Germany, 2008; pp. 57–76.

43. Pineda, J.N.B.; Bosque, S.J.; Gómez, D.M.; Plata, R.W. Análisis de cambio del uso del suelo en el Estado de México mediante sistemas de información geográfica y técnicas de regresión multivariantes: Una aproximación a los procesos de deforestación. *Investig. Geogr.* **2009**, *69*, 33–52.

44. Cano, S.L.; Rodríguez, L.R.; Valdez, L.J.R.; Acevedo, S.O.A.; Beltrán, H.R.I. Detección del crecimiento urbano en el estado de Hidalgo mediante imágenes Landsat. *Investig. Geogr.* **2017**, *92*, 1–10. [CrossRef]

45. Nájera, G.O.; Bojórquez, S.J.I.; Cifuentes, L.J.L.; Marceleño, F.S. Cambio de cobertura y uso del suelo en la cuenca del río Mololoa, Nayarit. *Revista Bio Ciencias* **2010**, *1*, 19–29. [CrossRef]